

LEARNING TO DIAGNOSE WITH LSTM RECURRENT NEURAL NETWORKS

Zachary C. Lipton *

Department of Computer Science and Engineering
 University of California, San Diego
 La Jolla, CA 92093, USA
 zlipton@cs.ucsd.edu

David C. Kale †

Department of Computer Science
 University of Southern California
 Los Angeles, CA 90089
 dkale@usc.edu

Charles Elkan

Department of Computer Science and Engineering
 University of California, San Diego
 La Jolla, CA 92093, USA
 elkan@cs.ucsd.edu

Randall Wetzel

Laura P. and Leland K. Whittier Virtual PICU
 Children’s Hospital Los Angeles
 Los Angeles, CA 90027
 rwetzel@chla.usc.edu

ABSTRACT

Clinical medical data, especially in the intensive care unit (ICU), consists of multivariate time series of observations. For each patient visit (or *episode*), sensor data and lab test results are recorded in the patient’s Electronic Health Record (EHR). While potentially containing a wealth of insights, the data is difficult to mine effectively, owing to varying length, irregular sampling and missing data. Recurrent Neural Networks (RNNs), particularly those using Long Short-Term Memory (LSTM) hidden units, are powerful and increasingly popular models for learning from sequence data. They adeptly model varying length sequences and capture long range dependencies. We present the first study to empirically evaluate the ability of LSTMs to recognize patterns in multivariate time series of clinical measurements. Specifically, we consider multilabel classification of diagnoses, training a model to classify 128 diagnoses given 13 frequently but irregularly sampled clinical measurements. First, we establish the effectiveness of a simple LSTM network for modeling clinical data. Then we demonstrate a straightforward and effective deep supervision strategy in which we replicate targets at each sequence step. Trained only on raw time series, our models outperforms several strong baselines on a wide variety of metrics, and nearly matches the performance of a multilayer perceptron trained on carefully hand-engineered features, establishing the usefulness of LSTMs for modeling medical data. The best LSTM model accurately classifies many diagnoses, including diabetic ketoacidosis (F1 score of .714), scoliosis (.677), and status asthmaticus (.632).

1 INTRODUCTION

Time series data comprised of clinical measurements, as recorded by caregivers in the pediatric intensive care unit (PICU), constitute an abundant and largely untapped source of medical insights. Potential uses of such data include classifying diagnoses accurately, predicting length of stay, predicting future illness, and predicting mortality. However, besides the difficulty of acquiring data, several obstacles stymie machine learning research with clinical time series. Episodes vary wildly in length, with stays ranging from just a few hours to multiple months. Observations, which include sensor data, vital signs, lab test results, and subjective assessments, are sampled irregularly, and are plagued by missing values (Marlin et al., 2012). Additionally, long-term time dependencies complicate learning with many algorithms. Lab results that taken together imply a particular diagnosis may be separated by days or weeks. Other examples of long-term dependencies include delays separating

* Author website: <http://zacklipton.com>

† Author website: <http://www-scf.usc.edu/~dkale/>

onsets of diseases from the appearance of symptoms. For example, symptoms of acute respiratory distress syndrome may not appear until 24-48 hours after lung injury (Mason et al., 2010).

Recurrent Neural Networks (RNNs), in particular those based on Long Short-Term Memory (LSTM) (Hochreiter & Schmidhuber, 1997), powerfully model varying-length sequential data, achieving state-of-the-art results for problems spanning natural language processing, image captioning, handwriting recognition, and genomic analysis (Auli et al., 2013; Sutskever et al., 2014; Vinyals et al., 2014; Karpathy & Fei-Fei, 2014; Liwicki et al., 2007; Graves et al., 2009; Pollastri et al., 2002; Vohradský, 2001; Xu et al., 2007). LSTMs can capture long range dependencies and nonlinear dynamics. Some sequence models, such as Markov models, conditional random fields, and Kalman filters, deal with sequential data but are ill-equipped to learn long-range dependencies. Other models require domain knowledge or feature engineering, offering less chance for serendipitous discovery. In contrast, neural networks learn representations and can discover unforeseen structure.

This paper presents the first empirical study of LSTMs applied to classifying diagnoses given multivariate PICU time series. Precisely, we formulate the problem as multilabel classification, since diagnoses are not mutually exclusive. Our examples are clinical episodes, each consisting of 13 frequently but irregularly sampled time series of clinical measurements, including body temperature, heart rate, diastolic and systolic blood pressure, and blood glucose among others. Associated with each patient are a subset of 429 diagnosis codes. As some are exceedingly rare, we focus on the 128 most common codes, classifying each episode with one or more diagnoses.

Because LSTMs have never been used in this setting, we methodically verify their utility. After first establishing set of strong baselines, we verify that even a simple LSTM architecture, trained to output predictions only at the final time step, beats a linear classifier when trained only on raw time series and nearly matches a MultiLayer Perceptron (MLP) trained on carefully hand-engineered features. We test a straightforward but novel target replication strategy for recurrent neural networks, inspired by the *deep supervision* technique of Lee et al. (2014) for training convolutional neural networks. We compose our optimization objective as a convex combination of the loss at the final sequence step and the mean of the losses over *all* sequence steps. Experiments demonstrate that target replication with a well-tuned hyper-parameter acts as a powerful regularizer, improving performance on all evaluation metrics. Finally, we evaluate the efficacy of using additional information in the patient’s chart as auxiliary outputs, a technique previously used with feed-forward nets (Caruana et al., 1996). We show that this too regularizes the model and that in combination with target replication, it yields even higher performance on some metrics.

2 RELATED WORK

Our research sits at the intersection of LSTMs, medical informatics, and multilabel classification, three well-developed fields, each with a long history and rich body of research. While we cannot possibly do justice to all three, we highlight the most relevant works below.

2.1 LSTM RNNs

LSTMs were originally introduced in Hochreiter & Schmidhuber (1997), following a long line of research into RNNs for sequence learning. Notable earlier work includes Elman (1990), which first used back-propagation through time to train recurrent neural networks to perform supervised machine learning. The design of modern LSTM memory cells has remained close to the original, with the commonly used additions of forget gates (Gers et al., 2000b) and peep-hole connections (Gers et al., 2000a). The connectivity pattern among multiple LSTM layers in our models follows the architecture described by Graves (2013). Pascanu et al. (2013) explores other mechanisms by which a recurrent neural network could be made *deep*. Surveys of the literature include Graves (2012), a thorough dissertation on sequence labeling with RNNs, De Mulder et al. (2015), which surveys natural language applications, and Lipton et al. (2015), which provides a broad overview of RNNs for sequence learning, focusing on modern applications.

2.2 NEURAL NETWORKS FOR MEDICAL DATA

Neural networks have been applied to medical problems and data for at least 20 years (Caruana et al., 1996; Baxt, 1995), although we know of no work on applying LSTMs to multivariate clinical time series of the type we analyze here. Several papers have applied RNNs to physiologic signals, including electrocardiograms (Silipo & Marchesi, 1998; Amari & Cichocki, 1998; Übeyli, 2009) and glucose measurements (Tresp & Briegel, 1998). RNNs have also been used for prediction problems in genomics (Pollastri et al., 2002; Xu et al., 2007; Vohradský, 2001). Multiple recent papers apply modern deep learning techniques (but not RNNs) to modeling psychological conditions (Dabek & Caban, 2015), head injuries (Rughani et al., 2010), and Parkinson’s disease (Hammerla et al., 2015). Recently, feed-forward networks have been applied to medical time series in sliding window fashion to discover meaningful patterns of physiology (Lasko et al., 2013; Che et al., 2015).

2.3 NEURAL NETWORKS FOR MULTILABEL CLASSIFICATION

Only a few published papers apply LSTMs to multilabel classification tasks, all of which, to our knowledge, are outside of the medical context. Liu et al. (2014) formulates music composition as a multilabel classification task, using sigmoidal output units. Most recently, Yeung et al. (2015) uses LSTM networks with multilabel outputs to recognize actions in videos. While we could not locate any published papers using LSTMs for multilabel classification in the medical domain, several papers use feed-forward nets for this task. One of the earliest papers to investigate multi-task neural networks modeled risk in pneumonia patients (Caruana et al., 1996). More recently, Che et al. (2015) formulated diagnosis as multilabel classification using a sliding window multilayer perceptron.

2.4 MACHINE LEARNING FOR CLINICAL TIME SERIES

Neural network methodology aside, a growing body of research applies machine learning to temporal clinical data for tasks including artifact removal (Aleks et al., 2009; Quinn et al., 2009), early detection and prediction (Stanculescu et al., 2014; Henry et al., 2015), and clustering and subtyping (Marlin et al., 2012; Schulam et al., 2015). Many recent papers use models with latent factors to capture nonlinear dynamics in clinical time series and to discover meaningful representations of health and illness. Gaussian processes and related techniques have proved popular because they can directly handle irregular sampling and encode prior knowledge via choice of covariance functions between time steps and across variables (Marlin et al., 2012; Ghassemi et al., 2015). Saria et al. (2010) combined a hierarchical dirichlet process with autoregressive models to infer latent disease “topics” in the heart rate signals of premature babies. Quinn et al. (2009) used linear dynamical systems with latent switching variables to model physiologic events like bradycardias. Citing inspiration from deep learning, Stanculescu et al. (2015) proposed models with a second “layer” of latent factors to capture correlations between latent states.

2.5 KEY DIFFERENCES

Our experiments show that LSTMs can successfully classify multivariate time series of clinical measurements, a topic not addressed in any prior work. Additionally, while some papers use LSTMs for multilabel classification, ours is the first to address this problem in the medical context. Moreover, for classifying varying length sequence with fixed length output vectors, this paper is the first, to our knowledge, to demonstrate the efficacy of a target replication strategy, achieving both faster training and better generalization.

3 DATA DESCRIPTION

Our experiments use a collection of fully anonymized clinical time series extracted from the EHR system at Children’s Hospital LA (Marlin et al., 2012; Che et al., 2015) as part of an IRB-approved study. The data consists of 10,401 PICU episodes, each a multivariate time series of 13 variables: diastolic and systolic blood pressure, peripheral capillary refill rate, end-tidal CO₂, fraction of inspired O₂, Glasgow coma scale, blood glucose, heart rate, pH, respiratory rate, blood oxygen saturation, body temperature, and urine output. Episodes vary in length from 12 hours to 30 days.

Each episode is associated with zero or more diagnostic labels from an in-house taxonomy used for research and billing, similar to codes from the *Ninth Revision of the International Classification of Diseases* (ICD-9) (World Health Organization, 2004). The dataset contains 429 distinct labels indicating a variety of conditions, such as acute respiratory distress, congestive heart failure, seizures, renal failure, and sepsis. Because many of the diagnoses are exceedingly rare, we focus on the most common 128, each of which occurs more than 50 times in the dataset.

The time series are irregularly sampled multivariate time series with both missing values and variables. We resample all time series to an hourly rate, taking the mean measurement within each one hour window. We use forward- and back-filling to fill gaps created by the window-based resampling. When a single variable’s time series is missing entirely, we impute a clinically normal value, as defined by clinical experts. These procedures make reasonable assumptions about clinical practice: many variables are recorded at rates proportional to how quickly they change, and when a variable is absent, it is often because clinicians believed it to be normal and chose not to measure it. Nonetheless, they are not appropriate in all settings. Back-filling, for example, passes information from the future backwards. This is acceptable for classifying entire episodes but not for forecasting.

We rescale all variables to $[0, 1]$ using ranges defined by clinical experts. We use published tables of normal values from large population studies to correct for differences in vital signs (e.g., blood pressure) that are due to age and gender (Fleming et al., 2011)(NHBPEP Working Group 2004).

4 METHODS

In this work, we are interested in recognizing diagnoses and, more broadly, the observable physiologic characteristics of patients, a task generally termed *phenotyping* (Oellrich et al., 2015). We cast the problem of phenotyping clinical time series as multilabel classification. Given a series of observations $\mathbf{x}^{(1)}, \dots, \mathbf{x}^{(T)}$, we learn a classifier to generate hypotheses $\hat{\mathbf{y}}$ of the true labels \mathbf{y} . Here, t indexes sequence steps, and for any example, T stands for the length of the sequence. Our proposed LSTM RNN uses memory cells with forget gates (Gers et al., 2000b) but without peephole connections (Gers et al., 2003). As output, we use a fully connected layer atop the highest LSTM layer followed by an element-wise sigmoid activation function, because our problem is multilabel. We use *log loss* as the loss function at each output.

The following equations give the update for a layer of memory cells $\mathbf{h}_l^{(t)}$ where $\mathbf{h}_{l-1}^{(t)}$ stands for the previous layer at the same sequence step (could be a previous LSTM layer or the input layer $\mathbf{x}^{(t)}$) and $\mathbf{h}_l^{(t-1)}$ stands for the same layer at the previous sequence step:

$$\begin{aligned} \mathbf{g}^{(t)} &= \phi(W_{\text{gx}}\mathbf{h}_{l-1}^{(t)} + W_{\text{gh}}\mathbf{h}_l^{(t-1)} + \mathbf{b}_g) \\ \mathbf{i}^{(t)} &= \sigma(W_{\text{ix}}\mathbf{h}_{l-1}^{(t)} + W_{\text{ih}}\mathbf{h}_l^{(t-1)} + \mathbf{b}_i) \\ \mathbf{f}^{(t)} &= \sigma(W_{\text{fx}}\mathbf{h}_{l-1}^{(t)} + W_{\text{fh}}\mathbf{h}_l^{(t-1)} + \mathbf{b}_f) \\ \mathbf{o}^{(t)} &= \sigma(W_{\text{ox}}\mathbf{h}_{l-1}^{(t)} + W_{\text{oh}}\mathbf{h}_l^{(t-1)} + \mathbf{b}_o) \\ \mathbf{s}^{(t)} &= \mathbf{g}^{(t)} \odot \mathbf{i}^{(t)} + \mathbf{s}^{(t-1)} \odot \mathbf{f}^{(t)} \\ \mathbf{h}_l^{(t)} &= \phi(\mathbf{s}^{(t)}) \odot \mathbf{o}^{(t)}. \end{aligned}$$

In these equations, σ stands for an element-wise application of the sigmoid function, ϕ stands for an element-wise application of the \tanh function and \odot is the Hadamard (element-wise) product. The input, output, and forget gates are denoted by \mathbf{i} , \mathbf{o} , and \mathbf{f} respectively, while \mathbf{g} is the input node and has a \tanh activation.

4.1 LSTM ARCHITECTURES FOR MULTILABEL CLASSIFICATION

We explore several recurrent neural network architectures for multilabel classification of time series. The first and simplest (Figure 1) passes over all inputs in chronological order, generating outputs only at the final sequence step. In this approach, we only have output $\hat{\mathbf{y}}$ at the final sequence step, at

which our loss function is the average of the losses at each output node. Thus the loss calculated at a single sequence step is the average of *log loss* calculated separately on each label.

$$\text{loss}(\hat{\mathbf{y}}, \mathbf{y}) = \frac{1}{|L|} \sum_{l=1}^{|L|} -(y_l \cdot \log(\hat{y}_l) + (1 - y_l) \cdot \log(1 - \hat{y}_l)).$$

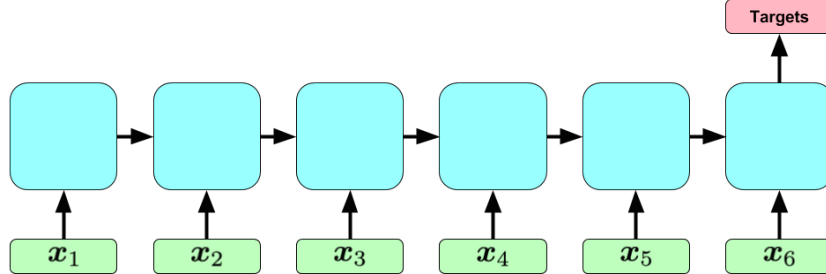


Figure 1: A simple RNN model for multilabel classification. Green rectangles represent inputs. The recurrent layer is depicted as a blue rectangle. The red rectangle represents targets.

4.2 SEQUENTIAL TARGET REPLICATION

One problem with the simple approach is that the network must learn to pass information across many sequence steps in order to affect the output. We attack this problem by replicating our static targets at each sequence step (Figure 2), providing intermediate targets offering a local error signal. This approach is partly inspired by the deep supervision technique that Lee et al. (2014) apply to convolutional nets. This technique is especially sensible in our case because we expect the model to predict accurately even if the sequence were truncated by a small amount. The approach differs from Lee et al. (2014) because we use the same output weights to calculate $\hat{\mathbf{y}}^{(t)}$ for all t . Further, we use this target replication to generate output at each sequence step, but not at each hidden layer.

For the model with target replication, we generate an output $\hat{\mathbf{y}}^{(t)}$ at every sequence step. Our loss is then a convex combination of the final loss with an average of the losses over all steps:

$$\alpha \cdot \frac{1}{T} \sum_{t=1}^T \text{loss}(\hat{\mathbf{y}}^{(t)}, \mathbf{y}^{(t)}) + (1 - \alpha) \cdot \text{loss}(\hat{\mathbf{y}}^{(T)}, \mathbf{y}^{(T)})$$

where T is the total number of sequence steps and $\alpha \in [0, 1]$ is a hyper-parameter which determines the relative importance of hitting these intermediary targets. At prediction time, we take only the output at the final step. In our experiments, networks using target replication outperformed those with a loss applied only on the final node in the sequence.

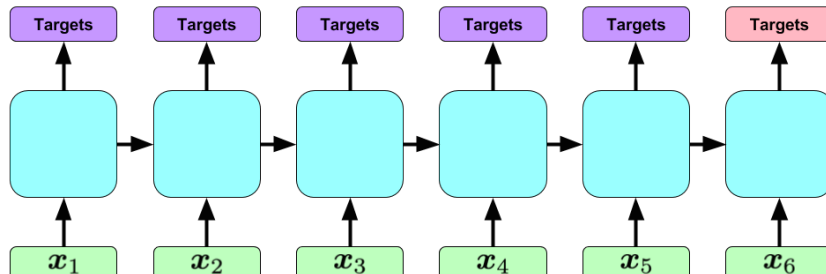


Figure 2: A recurrent neural network classification model with intermediate targets. The output (depicted in red) at the final step is used at prediction time, but at train time the model makes predictions (purple) at every sequence step.

5 JUNKOUT REGULARIZATION WITH AUXILIARY TARGETS

Recall that our initial data contained 429 diagnostic labels but that our task is to predict only 128. Given the well-documented successes of multitask learning with shared representations and feed-forward networks, it seems plausible that we can train a stronger model by using the remaining 301 labels or other information, such as diagnostic categories, as auxiliary targets (Caruana et al., 1996). These additional targets serve as regularizers: the model aims to minimize the loss on the labels of interest but must also learn representations that minimize loss on the auxiliary targets (Figure 3). Given the lower quality of some of the extra labels, we name this model “*JunkOut*.”

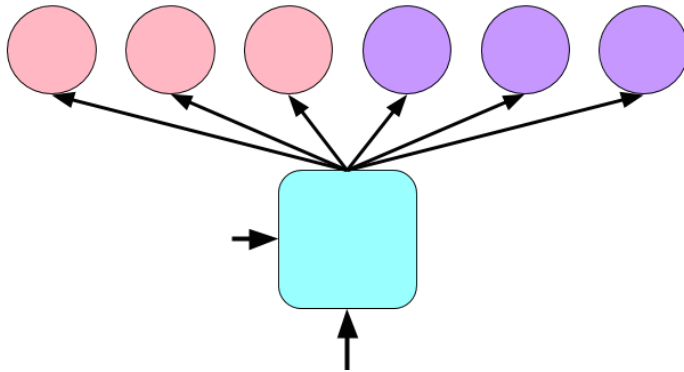


Figure 3: Our data-set contains many labels. For our task, a subset of 128 of them are of interest (depicted in red). Our *junkout* neural network makes use of all available additional labels as auxiliary training targets (depicted in purple). At inference time only the subset is used to generate output.

6 EXPERIMENTS

We train the network using stochastic gradient descent with momentum. Absent momentum, the variance of the gradient is large, and single examples can destroy the model. Interestingly, the presence of exploding gradients had no apparent connection to the loss on the particular example that caused it. To combat exploding gradients, we experimented with ℓ_2^2 weight decay, gradient clipping, and truncated back-propagation. Additionally, we found that deep supervision with target replication not only helped to learn faster but also served as a regularizer. In our final network, we used ℓ_2^2 regularization strength of 10^{-6} , deep supervision with $\alpha = 0.6$, hyperparameters which were chosen using validation data. Our final network used 2 hidden layers and 64 nodes per layer, an architecture also determined on the validation set. All models are trained on 80% of the data and tested on 10%. The remaining 10% is used as a validation set.

6.1 MULTILABEL EVALUATION METHODOLOGY

We report micro- and macro-averaged versions area under the ROC curve (AUC). By micro-AUC we mean a single AUC computed on flattened \hat{Y} and Y matrices, whereas macro-AUC is an average of the AUC computed separately for each label. The blind classifier achieves 0.5 macro-AUC but can exceed .5 on micro AUC by predicting labels in descending order by base rate. Additionally, we report micro- and macro- averaged F1 score. Similarly, micro is reported on flattened matrices and macro- is an average over the labels. F1 metrics require a thresholding strategy, and here we select thresholds based upon validation set performance. We refer to Lipton et al. (2014) for an analysis of the strengths and weaknesses of each multilabel F-score and a characterization of optimal thresholds.

Finally, we report *precision at 10*, which captures the fraction of true diagnoses among the model’s top 10 predictions, with a best possible score of 0.2281 on the test split of this data set because there are only 2.281 diagnoses per patient on average. While F1 and AUC are both useful for determining the relative quality of a classifier’s predictions, neither is tailored to a real-world application. Thus, we consider a medically plausible use case to motivate this more interpretable metric: generating a short list of the 10 most probable diagnoses. If we could create a high recall, moderate precision list

of 10 likely diagnoses, it could be a valuable hint-generation tool. Further, testing for only the 10 most probable conditions is much more realistic than testing for all conditions.

6.2 BASELINE CLASSIFIERS

We provide results for a *base rate* model that predicts diagnoses in descending order by incidence to provide a minimum performance baseline. We also report the performance of logistic regression, which is widely used in clinical research, training a separate classifier for each diagnosis and choosing L_2 regularization penalty on a validation set. For a much stronger baseline, we train an MLP with rectified linear activations, dropout of 0.5, and 3 hidden layers and 300 hidden nodes, hyperparameters chosen based on validation set performance. Each baseline is tested with two sets of inputs: raw time series and hand-engineered features. For raw time series, we used the first and last six hours. This provided classifiers with temporal information about changes in patient state from admission to discharge within a fixed-size input, as required by all baselines. We found this worked better than providing the first or last 12 hours. Our hand-engineered features are inspired by those used in state-of-the-art severity of illness scores (Pollack et al., 1996) and capture extremes (e.g., maximum), central tendencies (e.g., mean), variability, and trends. Such features have previously been shown to be very effective for these data (Marlin et al., 2012; Che et al., 2015).

6.3 RESULTS

LSTM models with two layers of 64 hidden units and trained with deep supervision (DS) performed best among models using only raw time series as inputs. **Table 1** shows a summary results for all models. All three DS models achieve Micro and Macro AUCs of over 0.84 and 0.78, respectively. We believe that there is further room for improvement, especially given access to a richer data set including a larger number of variables and treatment information. **Table 2** LSTM’s predictive performance for five critical care diagnoses with the highest F1 scores. Full per-diagnosis results may be found in **Appendix A**.

Deep supervision yielded substantial improvements over simple LSTMs on all metrics. It accelerated learning and allowed the model to continue improving for a larger number of epochs. Computing classification error at each step provides local targets to guide training, which may aid the LSTM-DS in modeling long-range interactions indicating changes in patient state. The performance of the MLP using the first and last six hours suggests the importance such interactions.

Overall classification performance for 128 ICU phenotypes using raw time series features					
Model	Micro AUC	Macro AUC	Micro F1	Macro F1	Prec. at 10
Base Rate	0.7128	0.5	0.1346	0.0343	0.0788
Logistic Regression, First 6 + Last 6	0.8074	0.7218	0.2221	0.1029	0.1021
MLP, First 6 + Last 6	0.8375	0.7770	0.2698	0.1286	0.1096
ML-LSTM	0.8300	0.7625	0.2611	0.1323	0.1093
ML-LSTM, JunkOut (Aux. labels)	0.8353	0.7703	0.2577	0.1333	0.1099
ML-LSTM, JunkOut (Categories)	0.8316	0.7671	0.2654	0.1251	0.1082
ML-LSTM-DS	0.8450	0.7842	0.2800	0.1365	0.1165
ML-LSTM-DS, JunkOut (Aux. labels)	0.8461	0.7926	0.2701	0.1414	0.1153
ML-LSTM-DS, JunkOut (Categories)	0.8461	0.7887	0.2818	0.1411	0.1136
Overall classification performance for 128 ICU phenotypes using hand-engineered features					
Logistic Regression	0.8286	0.7550	0.2515	0.1254	0.1111
MLP	0.8525	0.7990	0.2917	0.1468	0.1157

Table 1: Results on performance metrics calculated across all labels.

Using additional targets (“JunkOut”) improved performance for most metrics, and reduced overfitting, but the effect was less dramatic than for deep supervision. Additionally, these gains came at the cost of slower training: the JunkOut models required more epochs, especially when using the 300 auxiliary labels. This may be due in part to class imbalance. For many of these labels it may take an entire epoch just to learn that they are occasionally nonzero.

The best performing model in our experiments was an MLP using hand-engineered features as input. This is not surprising as this model is able to directly exploit domain knowledge and features like

variability and trends that the LSTMs must learn. The LSTMs with deep supervision surpass the MLP on all metrics when both are trained on raw features.

Best 5 Labels measured by F1				
Label	AUC	F1	Precision	Recall
Diabetic Ketoacidosis	0.8995	0.7143	0.9091	0.5882
Scoliosis	0.8646	0.6763	0.6596	0.6940
Asthma - Status Asthmaticus	0.9439	0.6315	0.9230	0.48
Cerebral Tumor	0.8357	0.4866	0.4025	0.6153
Acute Respiratory Failure	0.8646	0.4429	0.3604	0.5741

Table 2: Results on performance metrics calculated on the 5 labels with highest F1.

7 DISCUSSION

Our results indicate that LSTM RNNs, especially when provided with deep supervision in the form of target replication, can successfully classify diagnoses of critical care patients given clinical time series data. Our experiments demonstrate a clear advantage over all linear baselines and over traditional feedforward architectures applied to raw measurements. However, this is only a first step in this line of research. Recognizing current diagnoses given only sensor data demonstrates that LSTMs can capture meaningful signal, but ultimately we would like to accurately predict unknown conditions and events, including outcomes such as mortality and treatment responses. In this work we used diagnostic labels without timestamps, but we are working to obtain time-stamped diagnoses, which would enable us to train models to perform early diagnosis by predicting future conditions. On the strength of these results, we are currently extending this work to a larger PICU data set with a richer set of measurements, including treatments and medications.

On the methodological side, we would like to both improve and better exploit the capabilities of LSTMs. Results from speech recognition have shown that LSTMs shine in comparison to other models using raw features. In the clinical setting, LSTMs may allow us to exploit previously difficult to mine sources of data while minimizing the preprocessing and feature engineering required. In contrast, our current data preparation pipeline removes valuable structure and information from clinical time series that could be exploited by a LSTM. For example, our forward- and back-filling imputation strategies discard useful information about which observations were recorded when. Imputing normal values for missing time series ignores the meaningful distinction between truly normal and missing measurements. In future work, we plan to introduce indicator variables to allow the LSTM to distinguish actual from missing or imputed measurements. Also, our window-based resampling procedure reduces the variability of more frequently measured vital signs (e.g., heart rate). The flexibility of the LSTM architecture should also enable us to eliminate age-based corrections and to incorporate non-sequential inputs, such as age, weight, and height (or even hand-engineered features), into predictions.

Next steps in this direction include developing LSTM architectures to directly handle missing values and irregular sampling. We also are encouraged by the success of target replication and plan to explore other variants of this technique and to apply it to other domains and tasks. Additionally, we acknowledge that there remains a debate about the interpretability of neural networks when applied to complex medical problems. We are developing methods to interpret the representations learned by LSTMs in order to better expose patterns of health and illness to clinical users. We also hope to make practical use of the distributed representations of patients for patient similarity search.

8 ACKNOWLEDGEMENTS

Zachary C. Lipton was supported by the Division of Biomedical Informatics at the University of California, San Diego, via training grant (T15LM011271) from the NIH/NLM. David Kale was supported by the Alfred E. Mann Innovation in Engineering Doctoral Fellowship. The VPICU was supported by grants from the Laura P. and Leland K. Whittier Foundation. We acknowledge NVIDIA Corporation for Tesla K40 GPU hardware donation and Professors Julian McAuley and Greg Ver Steeg for their support and advice.

REFERENCES

Aleks, Norm, Russell, Stuart J, Madden, Michael G, Morabito, Diane, Staudemayer, Kristan, Cohen, Mitchell, and Manley, Geoffrey T. Probabilistic detection of short events, with application to critical care monitoring. In *Advances in Neural Information Processing Systems*, pp. 49–56, 2009.

Amari, Shun-ichi and Cichocki, Andrzej. Adaptive blind signal processing-neural network approaches. *Proceedings of the IEEE*, 86(10):2026–2048, 1998.

Auli, Michael, Galley, Michel, Quirk, Chris, and Zweig, Geoffrey. Joint language and translation modeling with recurrent neural networks. In *EMNLP*, volume 3, pp. 0, 2013.

Baxt, W.G. Application of artificial neural networks to clinical medicine. *The Lancet*, 346(8983): 1135–1138, 1995. ISSN 0140-6736.

Caruana, Rich, Baluja, Shumeet, Mitchell, Tom, et al. Using the future to “sort out” the present: Rankprop and multitask learning for medical risk evaluation. *Advances in neural information processing systems*, pp. 959–965, 1996.

Che, Zhengping, Kale, David C., Li, Wenzhe, Bahadori, Mohammad Taha, and Liu, Yan. Deep computational phenotyping. In *Proceedings of the 21th ACM SIGKDD International Conference on Knowledge Discovery and Data Mining*, KDD ’15, pp. 507–516, New York, NY, USA, 2015. ACM. ISBN 978-1-4503-3664-2. doi: 10.1145/2783258.2783365. URL <http://doi.acm.org/10.1145/2783258.2783365>.

Dabek, Filip and Caban, Jesus J. A neural network based model for predicting psychological conditions. In *Brain Informatics and Health*, pp. 252–261. Springer, 2015.

De Mulder, Wim, Bethard, Steven, and Moens, Marie-Francine. A survey on the application of recurrent neural networks to statistical language modeling. *Computer Speech & Language*, 30(1): 61–98, 2015.

Elman, Jeffrey L. Finding structure in time. *Cognitive Science*, 14(2):179–211, 1990.

Fleming, Susannah, Thompson, Matthew, Stevens, Richard, Heneghan, Carl, Plddemann, Annette, Maconochie, Ian, Tarassenko, Lionel, and Mant, David. Normal ranges of heart rate and respiratory rate in children from birth to 18 years: A systematic review of observational studies. *Lancet*, pp. 1011–1018, 2011.

Gers, Felix, Schmidhuber, Jürgen, et al. Recurrent nets that time and count. In *Neural Networks, 2000. IJCNN 2000, Proceedings of the IEEE-INNS-ENNS International Joint Conference on*, volume 3, pp. 189–194. IEEE, 2000a.

Gers, Felix A., Schmidhuber, Jürgen, and Cummins, Fred. Learning to forget: Continual prediction with LSTM. *Neural Computation*, 12(10):2451–2471, 2000b.

Gers, Felix A., Schraudolph, Nicol N., and Schmidhuber, Jürgen. Learning precise timing with lstm recurrent networks. *The Journal of Machine Learning Research*, 3:115–143, 2003.

Ghassemi, Marzyeh, Pimentel, Marco AF, Naumann, Tristan, Brennan, Thomas, Clifton, David A, Szolovits, Peter, and Feng, Mengling. A multivariate timeseries modeling approach to severity of illness assessment and forecasting in ICU with sparse, heterogeneous clinical data. In *Proc. Twenty-Ninth AAAI Conf. on Artificial Intelligence*, 2015.

Graves, Alex. *Supervised sequence labelling with recurrent neural networks*, volume 385. Springer, 2012.

Graves, Alex. Generating sequences with recurrent neural networks. *arXiv preprint arXiv:1308.0850*, 2013.

Graves, Alex, Liwicki, Marcus, Fernández, Santiago, Bertolami, Roman, Bunke, Horst, and Schmidhuber, Jürgen. A novel connectionist system for unconstrained handwriting recognition. *Pattern Analysis and Machine Intelligence, IEEE Transactions on*, 31(5):855–868, 2009.

Hammerla, Nils Y, Fisher, James M, Andras, Peter, Rochester, Lynn, Walker, Richard, and Plötz, Thomas. Pd disease state assessment in naturalistic environments using deep learning. In *Proc. Twenty-Ninth AAAI Conf. on Artificial Intelligence*, 2015.

Henry, Katharine E, Hager, David N, Pronovost, Peter J, and Saria, Suchi. A targeted real-time early warning score (trewscore) for septic shock. *Science Translational Medicine*, 7(299):299ra122–299ra122, 2015.

Hochreiter, Sepp and Schmidhuber, Jürgen. Long short-term memory. *Neural Computation*, 9(8):1735–1780, 1997.

Karpathy, Andrej and Fei-Fei, Li. Deep visual-semantic alignments for generating image descriptions. *arXiv preprint arXiv:1412.2306*, 2014.

Lasko, Thomas A., Denny, Joshua C., and Levy, Mia A. Computational phenotype discovery using unsupervised feature learning over noisy, sparse, and irregular clinical data. *PLoS ONE*, 8(6):e66341, 06 2013. doi: 10.1371/journal.pone.0066341.

Lee, Chen-Yu, Xie, Saining, Gallagher, Patrick, Zhang, Zhengyou, and Tu, Zhuowen. Deeply-supervised nets. *arXiv preprint arXiv:1409.5185*, 2014.

Lipton, Zachary C, Elkan, Charles, and Narayanaswamy, Balakrishnan. Optimal thresholding of classifiers to maximize f1 measure. In *Machine Learning and Knowledge Discovery in Databases*, pp. 225–239. Springer, 2014.

Lipton, Zachary C., Berkowitz, John, and Elkan, Charles. A critical review of recurrent neural networks for sequence learning. *arXiv preprint arXiv:1506.00019*, 2015.

Liu, I, Ramakrishnan, Bhiksha, et al. Bach in 2014: Music composition with recurrent neural network. *arXiv preprint arXiv:1412.3191*, 2014.

Liwicki, Marcus, Graves, Alex, Bunke, Horst, and Schmidhuber, Jürgen. A novel approach to on-line handwriting recognition based on bidirectional long short-term memory networks. In *Proc. 9th Int. Conf. on Document Analysis and Recognition*, volume 1, pp. 367–371, 2007.

Marlin, Ben M., Kale, David C., Khemani, Robinder G., and Wetzel, Randall C. Unsupervised pattern discovery in electronic health care data using probabilistic clustering models. In *IHI*, 2012.

Mason, Robert J., Broaddus, V. Courtney, Martin, Thomas, King Jr., Talmadge E., Schraufnagel, Dean, Murray, John F., and Nadel, Jay A. *Murray and Nadel's textbook of respiratory medicine: 2-volume set*. Elsevier Health Sciences, 2010.

National High Blood Pressure Education Program Working Group on Children and Adolescents. The fourth report on the diagnosis, evaluation, and treatment of high blood pressure in children and adolescents. *Pediatrics*, 114:555–576, 2004.

Oellrich, Anika, Collier, Nigel, Groza, Tudor, Rebholz-Schuhmann, Dietrich, Shah, Nigam, Bodenreider, Olivier, Boland, Mary Regina, Georgiev, Ivo, Liu, Hongfang, Livingston, Kevin, Luna, Augustin, Mallon, Ann-Marie, Manda, Prashanti, Robinson, Peter N., Rustici, Gabriella, Simon, Michelle, Wang, Liqin, Winnenburg, Rainer, and Dumontier, Michel. The digital revolution in phenotyping. *Briefings in Bioinformatics*, 2015. doi: 10.1093/bib/bbv083.

Pascanu, Razvan, Gulcehre, Caglar, Cho, Kyunghyun, and Bengio, Yoshua. How to construct deep recurrent neural networks. *arXiv preprint arXiv:1312.6026*, 2013.

Pollack, M. M., Patel, K. M., and Ruttimann, U. E. *PRISM III: an updated Pediatric Risk of Mortality score*. *Critical Care Medicine*, 24(5):743–752, 1996.

Pollastri, Gianluca, Przybylski, Darisz, Rost, Burkhard, and Baldi, Pierre. Improving the prediction of protein secondary structure in three and eight classes using recurrent neural networks and profiles. *Proteins: Structure, Function, and Bioinformatics*, 47(2):228–235, 2002.

Quinn, John, Williams, Christopher KI, McIntosh, Neil, et al. Factorial switching linear dynamical systems applied to physiological condition monitoring. *Pattern Analysis and Machine Intelligence, IEEE Transactions on*, 31(9):1537–1551, 2009.

Rughani, Anand I., Dumont, Travis M., Lu, Zhenyu, Bongard, Josh, Horgan, Michael A., Penar, Paul L., and Tranmer, Bruce I. Use of an artificial neural network to predict head injury outcome: clinical article. *Journal of neurosurgery*, 113(3):585–590, 2010.

Saria, Suchi, Koller, Daphne, and Penn, Anna. Learning individual and population level traits from clinical temporal data. In *Proc. Neural Information Processing Systems (NIPS), Predictive Models in Personalized Medicine workshop*. Citeseer, 2010.

Schulam, Peter, Wigley, Fredrick, and Saria, Suchi. Clustering longitudinal clinical marker trajectories from electronic health data: Applications to phenotyping and endotype discovery. In *Twenty-Ninth AAAI Conference on Artificial Intelligence*, 2015.

Silipo, Rosaria and Marchesi, Carlo. Artificial neural networks for automatic ecg analysis. *Signal Processing, IEEE Transactions on*, 46(5):1417–1425, 1998.

Stanculescu, Ioan, Williams, Christopher K, Freer, Yvonne, et al. Autoregressive hidden markov models for the early detection of neonatal sepsis. *Biomedical and Health Informatics, IEEE Journal of*, 18(5):1560–1570, 2014.

Stanculescu, Ioan, Williams, Christopher KI, and Freer, Yvonne. A hierarchical switching linear dynamical system applied to the detection of sepsis in neonatal condition monitoring. 2015.

Sutskever, Ilya, Vinyals, Oriol, and Le, Quoc VV. Sequence to sequence learning with neural networks. In *Advances in Neural Information Processing Systems*, pp. 3104–3112, 2014.

Tresp, Volker and Briegel, Thomas. A solution for missing data in recurrent neural networks with an application to blood glucose prediction. In Jordan, M.I., Kearns, M.J., and Solla, S.A. (eds.), *Advances in Neural Information Processing Systems 10*, pp. 971–977. MIT Press, 1998.

Übeyli, Elif Derya. Combining recurrent neural networks with eigenvector methods for classification of ecg beats. *Digital Signal Processing*, 19(2):320–329, 2009.

Vinyals, Oriol, Toshev, Alexander, Bengio, Samy, and Erhan, Dumitru. Show and tell: A neural image caption generator. *arXiv preprint arXiv:1411.4555*, 2014.

Vohradský, Jiří. Neural network model of gene expression. *The FASEB Journal*, 15(3):846–854, 2001.

World Health Organization. *International statistical classification of diseases and related health problems*, volume 1. World Health Organization, 2004.

Xu, Rui, Wunsch II, Donald, and Frank, Ronald. Inference of genetic regulatory networks with recurrent neural network models using particle swarm optimization. *IEEE/ACM Transactions on Computational Biology and Bioinformatics (TCBB)*, 4(4):681–692, 2007.

Yeung, Serena, Russakovsky, Olga, Jin, Ning, Andriluka, Mykhaylo, Mori, Greg, and Fei-Fei, Li. Every moment counts: Dense detailed labeling of actions in complex videos. *arXiv preprint arXiv:1507.05738*, 2015.

Appendices

A PER DIAGNOSIS RESULTS

Classifier Performance on Each Diagnostic Code Sorted by AUC					
Label	AUC	AUPRC	F1	Precision	Recall
Asthma	0.9439	0.7657	0.6315	0.9230	0.48
Child abuse	0.9434	0.1278	0.1	0.1111	0.0909
Pulmonary Congestion and hypostasis	0.9386	0.0502	0.0833	0.0476	0.3333
Respiratory Syncytial Virus	0.9376	0.2047	0.2222	0.2142	0.2307
Pneumonia due to adenovirus	0.9355	0.0944	0.1621	0.1034	0.375
Bronchiolitis due to other infectious organism	0.9293	0.2829	0.2051	0.2352	0.1818
Agranulocytosis	0.9259	0.0637	0.1081	0.0689	0.25
Acute Pericarditis	0.9232	0.0639	0.0952	0.0833	0.1111
Extradural hemorrhage following injury w/out open wound	0.9222	0.0682	0.1081	0.0740	0.2
Biliary atresia	0.9220	0.1967	0.0421	0.0224	0.3333
Anoxic brain damage	0.9184	0.0789	0.1230	0.0740	0.3636
Failure	0.9169	0.3042	0.4137	0.5	0.3529
Defibrillation syndrome	0.9159	0.1617	0.24	0.25	0.2307
Renal transplant status post	0.9141	0.2893	0.1818	0.1025	0.8
Insufficiency	0.9121	0.3285	0.3076	0.2352	0.4444
Liver transplant status post	0.9111	0.0392	0.0740	0.0416	0.3333
Acidosis	0.9025	0.1633	0.2857	0.4	0.2222
Injury to multiple and unspecified intrathoracic organs	0.9010	0.1185	0.0176	0.0089	0.8
Anomalies of the skull and face bone	0.9009	0.3725	0.0346	0.0177	0.7142
Diabetes mellitus with ketoacidosis	0.8994	0.7817	0.7142	0.9090	0.5882
Neurofibromatosis	0.8985	0.0498	0.0909	0.0666	0.1428
Unspecified pleural effusion	0.8963	0.1980	0.0869	0.05	0.3333
Septic Shock	0.8905	0.2792	0.3838	0.2714	0.6551
Lung Contusion w/out open wound	0.8862	0.0405	0.0333	0.0196	0.1111
Congenital hereditary muscular dystrophy	0.8800	0.1636	0.3333	0.2727	0.4285
Werdnig-Hoffman Disease	0.8786	0.0671	0.0	0.0	0.0
Infantile cerebral palsy	0.8754	0.2176	0.2857	0.2903	0.2812
Scoliosis	0.8646	0.7055	0.6763	0.6595	0.6940
Pneumonia due to inhalation of food or vomitus	0.8622	0.0442	0.0888	0.0606	0.1666
Grand mal status	0.8600	0.2155	0.3010	0.2333	0.4242
Acute renal failure	0.8596	0.1796	0.3043	0.2916	0.3181
Benign intracranial hypertension	0.8517	0.1409	0.1276	0.0833	0.2727
End Stage Renal Disease on dialysis	0.8514	0.4408	0.4285	0.3333	0.6
Coma	0.8501	0.0843	0.0229	0.0116	0.8888
Acute Pancreatitis	0.8487	0.0898	0.0833	0.0447	0.6
Mycoplasma pneumoniae	0.8456	0.0842	0.1842	0.1186	0.4117
Pulmonary hypertension	0.8433	0.1489	0.0975	0.0547	0.4444
Unspecified disorder of kidney and ureter	0.8427	0.2282	0.3333	0.28	0.4117
Congenital heart disease	0.8385	0.0581	0.1379	0.1	0.2222
Chronic Respiratory disease arising in the perinatal period	0.8383	0.1387	0.2077	0.1777	0.25
Neoplasm	0.8357	0.4464	0.4866	0.4025	0.6153
Hypertension	0.8326	0.0729	0.0917	0.05	0.5555
Intracranial injury	0.8324	0.2704	0.3	0.2330	0.4210
Cardiac Arrest - Outside Hospital	0.8280	0.2598	0.0421	0.0215	0.9523
Acute lymphoid leukemia	0.8279	0.0945	0.1470	0.0884	0.4347
Cerebral edema	0.8263	0.0764	0.015	0.0075	0.6
Pneumococcal pneumonia	0.8249	0.0890	0.1754	0.1351	0.25
Other spontaneous pneumothorax	0.8236	0.0494	0.0941	0.0540	0.3636
Diabetes insipidus	0.8225	0.0900	0.15	0.1111	0.2307
Intracranial hemorrhage	0.8216	0.1468	0.1470	0.0892	0.4166
Cerebral artery occlusion	0.8139	0.0163	0.0256	0.0134	0.2857

Table 3: Results on performance metrics calculated on the 5 labels with highest F1.

(continued) Classifier Performance on Each Diagnostic Code Sorted by AUC					
Label	AUC	AUPRC	F1	Precision	Recall
Pneumonia	0.8139	0.0876	0.1463	0.1	0.2727
Injury to unspecified intra-abdominal organs	0.8101	0.1986	0.0408	0.0212	0.5
Septicemia NOS	0.8097	0.1589	0.1686	0.1076	0.3888
Respiratory complications resulting from a procedure	0.8068	0.2027	0.2388	0.25	0.2285
Cystic Fibrosis with pulmonary manifestations	0.8059	0.1197	0.0320	0.0164	0.6
Acute Respiratory Failure	0.8057	0.3235	0.4428	0.3604	0.5740
Encephalopathy NOS	0.7991	0.0410	0.1428	0.25	0.1
Arteriovenous malformation of the brain	0.7984	0.1900	0.2448	0.24	0.25
Apnea	0.7978	0.1033	0.1111	0.1333	0.0952
Malignant neoplasm	0.7902	0.0274	0.0361	0.0192	0.3
Disorder of Muscle NEC	0.7894	0.1847	0.0347	0.0178	0.6363
Other Shock	0.7889	0.0257	0.0545	0.03	0.3
Diabetes mellitus	0.7861	0.0775	0.1333	0.125	0.1428
Motor vehicle accident involving collision w/ another motor vehicle	0.7853	0.0864	0.1506	0.0956	0.3548
Less than 37 weeks gestation	0.7847	0.1304	0.1981	0.1594	0.2619
Conditions due to anomaly of unspecified circumstance	0.7823	0.2163	0.25	0.4285	0.1764
Other respiratory symptom	0.7814	0.2565	0.3333	0.2807	0.4102
Supraventricular premature beats	0.7813	0.0455	0.0952	0.0714	0.1428
Anomalies of the skull and face bone	0.7797	0.0617	0.1428	0.125	0.1666
Cardiac dysrhythmia	0.7795	0.1699	0.125	0.1428	0.1111
Other diseases of the respiratory system	0.7792	0.1467	0.2020	0.2127	0.1923
Obesity	0.7777	0.0418	0.0661	0.0366	0.3333
Hematemesis	0.7761	0.0129	0.0191	0.0097	0.6
Pneumonitis due to inhalation of food or vomitus	0.7756	0.0222	0.0476	0.0256	0.3333
Congenital hydrocephalus	0.7752	0.1847	0.2432	0.3	0.2045
Fracture	0.7739	0.1425	0.0740	0.0625	0.0909
Other primary cardiomyopathies	0.7652	0.2835	0.2666	0.2727	0.2608
Hyposmolality and/or hyponatremia	0.7638	0.0104	0.0176	0.0090	0.4
Other and unspecified coagulation defects	0.7635	0.1154	0.1086	0.0657	0.3125
null	0.7615	0.0389	0.0701	0.0384	0.4
Epilepsy	0.7584	0.3188	0.3873	0.3282	0.4725
Mechanical complication of V-P shunt	0.7580	0.0203	0.1	0.0833	0.125
Delayed milestones	0.7564	0.3421	0.3944	0.3467	0.4574
Esophageal reflux	0.7545	0.0585	0.1234	0.0833	0.2380
Croup Syndrome	0.7538	0.0403	0.0165	0.0083	0.7142
Heart Disease	0.7526	0.0426	0.0769	0.0666	0.0909
Subdural hemorrhage following injury w/out open wound	0.7477	0.0553	0.0810	0.0535	0.1666
Malignant neoplasm	0.7431	0.0101	0.0152	0.0078	0.3333
History of surgery to major organs	0.7429	0.0474	0.0454	0.0270	0.1428
Congenital Central Alveolar Hypoventilation Syndrome	0.7400	0.0127	0.0095	0.0049	0.1428
Acute and subacute necrosis of the liver	0.7383	0.1321	0.1904	0.1666	0.2222
Anemia	0.7321	0.0388	0.0327	0.0173	0.2857
Dehydration	0.7319	0.0360	0.0888	0.0588	0.1818
Unspecified disease of spinal cord	0.7291	0.0614	0.0720	0.0421	0.25
Primary Malignant neoplasm	0.7274	0.0170	0.0270	0.0141	0.3
Urinary Tract Infection	0.7259	0.0491	0.0941	0.0579	0.25
Malignancy of bone - no site specified	0.7184	0.0180	0.0833	0.0487	0.2857
Drowning and non-fatal submersion	0.7174	0.0146	0.0272	0.0142	0.2857
Observation of newborn and infant for suspected condition not found	0.7169	0.0347	0.0683	0.04	0.2352
Insomnia with sleep apnea	0.7108	0.2015	0.0961	0.0574	0.2941
Bone Marrow Transplant Status	0.7077	0.0770	0.0983	0.0588	0.3
Thrombocytopenia	0.7060	0.0209	0.0512	0.0280	0.3
Unspecified Intestinal obstruction	0.7045	0.0495	0.0638	0.0379	0.2
Unspecified injury	0.7020	0.0333	0.0	0.0	0.0
Unspecified disorder of intestine	0.6961	0.0550	0.075	0.0468	0.1875
Blood in stool	0.6908	0.0089	0.0245	0.0127	0.3333
Respiratory Arrest	0.6883	0.1622	0.1052	0.0833	0.1428
Malignant neoplasm	0.6790	0.0590	0.0486	0.0254	0.5333
Panhypopituitarism	0.6784	0.0146	0.0242	0.0127	0.25
Other complications of nervous system device	0.6760	0.0132	0.0289	0.0153	0.25
Ostium secundum type atrial septal defect	0.6750	0.0218	0.0437	0.0234	0.3333
Hereditary hemolytic anemia	0.6733	0.0115	0.0262	0.0135	0.4285

(continued) Classifier Performance on Each Diagnostic Code Sorted by AUC					
Label	AUC	AUPRC	F1	Precision	Recall
Sickle-cell anemia	0.6712	0.0093	0.0263	0.0134	0.6
Ventricular septal defect	0.6580	0.0170	0.0444	0.025	0.2
Other specified cardiac dysrhythmia	0.6554	0.0483	0.0168	0.0086	0.3333
Conditions due to anomaly of unspecified circumstance	0.6537	0.0991	0.1637	0.1031	0.3965
Injury crushing NOS	0.6445	0.0085	0.0191	0.0098	0.4
Respiratory complications resulting from a procedure	0.6385	0.0275	0.0291	0.0157	0.2
Hemophilus meningitis	0.6240	0.0080	0.0135	0.0068	0.3333
HEMATOLOGIC - Other	0.6078	0.0212	0.0394	0.0215	0.2352
Unspecified disorder of thyroid	0.6068	0.0182	0.0151	0.0077	0.375
Disorders Of The Nervous System	0.5847	0.0315	0.0553	0.0290	0.5652
Unspecified disorder of immune mechanism	0.5658	0.0205	0.0377	0.0208	0.2
Unspecified disorder of metabolism	0.5552	0.0313	0.0555	0.0454	0.0714
GI SURGERY - Other	0.5412	0.0152	0.0241	0.0129	0.1875
Asthma NOS	0.5398	0.0168	0.0335	0.0175	0.4117
Tetralogy of Fallot	0.4325	0.0058	0.0082	0.0042	0.2857